Supplementary Figures

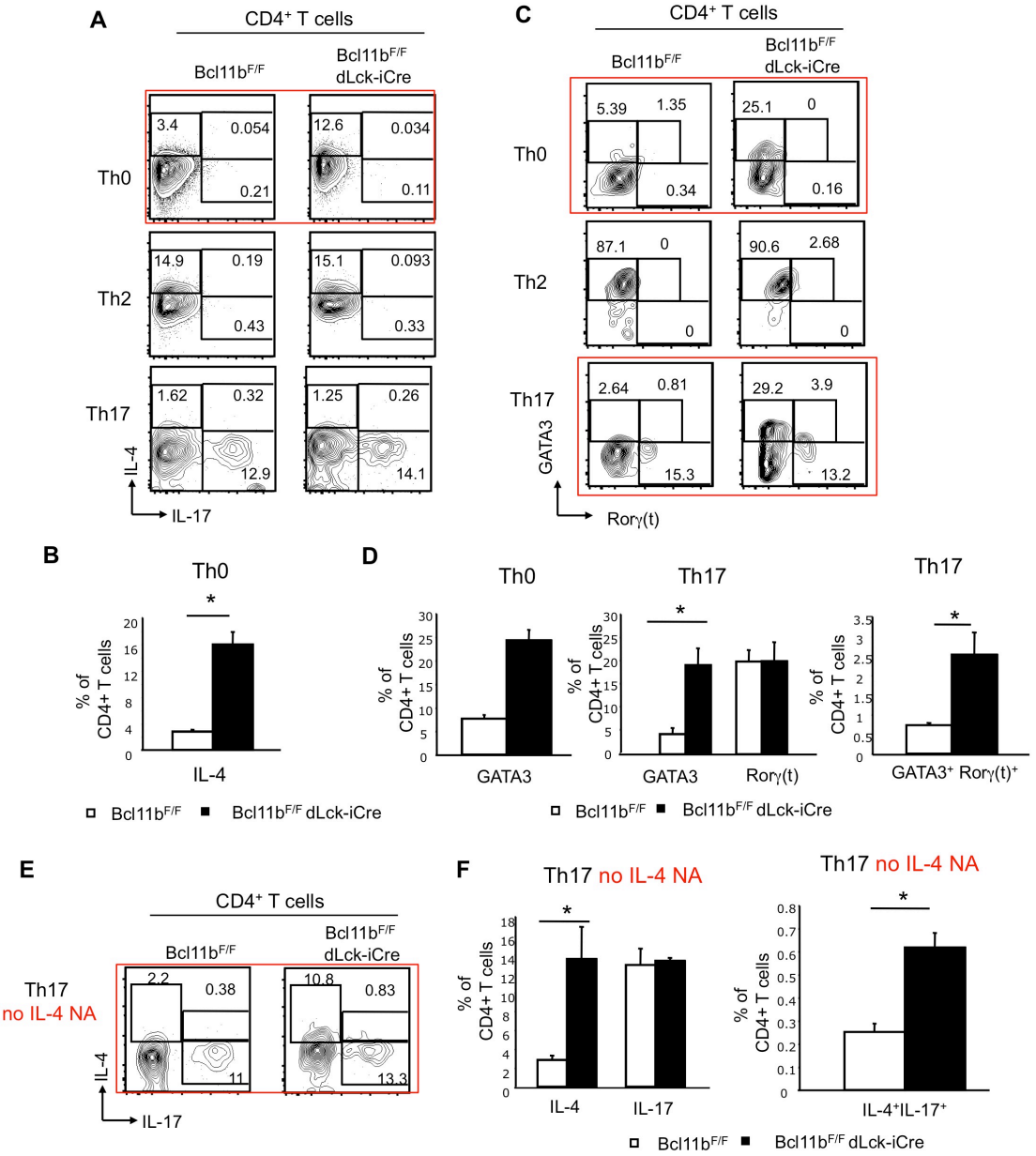

Figure S1. Levels of GATA3 and IL-4 are elevated in Th0 conditions and remain unrepressed in Th17-polarized CD4$^+$ T cells when Bcl11b is deficient. Purified CD4$^+$ T cells from Bcl11b$^{F/F}$dLck-iCre and wild type mice were cultured on anti-CD3-coated plates plus soluble anti-CD28, in Th0, Th2 or Th17 polarizing conditions, as described in Supplemental Methods. (A) Evaluation of lineage-specific cytokines by FACS analysis. (B) Average frequency of IL-4$^+$CD4$^+$ T cells in Th0 polarized cells,*p≤0.05, n=6 (mean ±SEM). (C) Evaluation of lineage-specific transcription factors by FACS analysis. (D) Average frequencies of GATA3$^+$CD4$^+$ T cells in Th0 polarized cells (left), GATA3$^+$CD4$^+$ or Rorγt$^+$CD4$^+$ T cells in Th17 polarized cells (center), and GATA3$^+$Rorγt$^+$CD4$^+$ T cells in Th17 polarized cells (right), *p≤0.05, n=6 (mean ±SEM). (E) Evaluation of IL-17 and IL-4 in CD4$^+$ T cells polarized in Th17 conditions without inhibitory antibodies for IL-4 by FACS analysis. (F) Average frequencies of IL-4$^+$ or IL-17$^+$ (left) and IL-4$^+$IL-17$^+$ (right) CD4$^+$ T cells in Th17 conditions without inhibitory antibodies for IL-4,*p≤0.05, n=6 (mean ±SEM). Significance was determined by two-tailed student's *t* test. Red boxes indicate abnormal IL-4 production. Data is representative of six independent experiments.

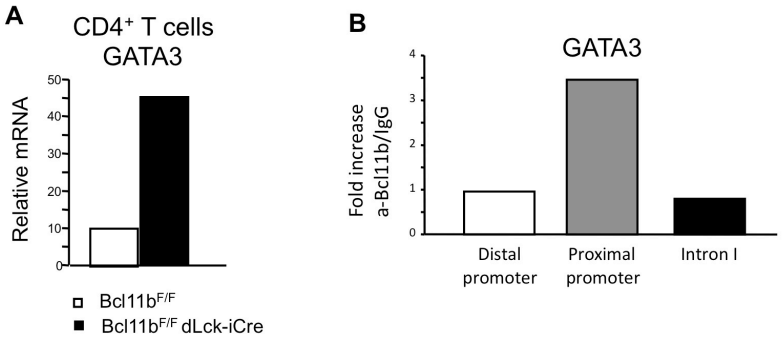

Figure S2. Bcl11b associates with the proximal promoter in the GATA3 locus. (A) Quantitative RT-PCR analysis of GATA3 mRNA levels in $CD4^+$ T cells from $Bcl11b^{F/F}$/dLck-iCre (black) and wild type (white) mice on day 12 after EAE induction. Data is derived from three independent experiments with two mice per group. (B) Chromatin immunoprecipitation (ChIP) of cross-linked nuclear extracts from purified $CD4^+$ T cells, by anti-Bcl11b or IgG (control) antibodies. ChIP-ed DNA was amplified by quantitative PCR with primers for GATA3 proximal promoter (gray), distal promoter region (white), or a conserved region in intron I (black). Bcl11b-ChIP-ed DNA was normalized to the input in each case and expressed as fold increase over IgG.

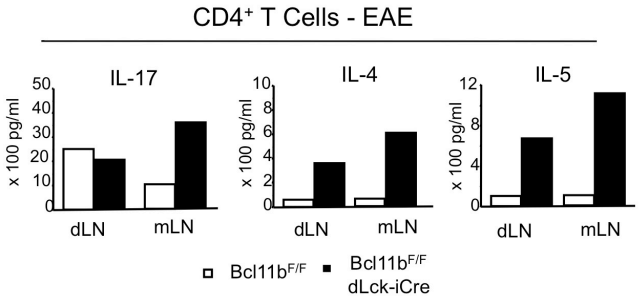

Figure S3. Luminex assays of IL-17, IL-4 and IL-5 cytokines produced by purified CD4$^+$ T cells of Bcl11b$^{F/F}$/dLck-iCre (black) and wild type (white) mice on day 12 after EAE induction. Data is representative for two independent experiments with four pairs of mice.

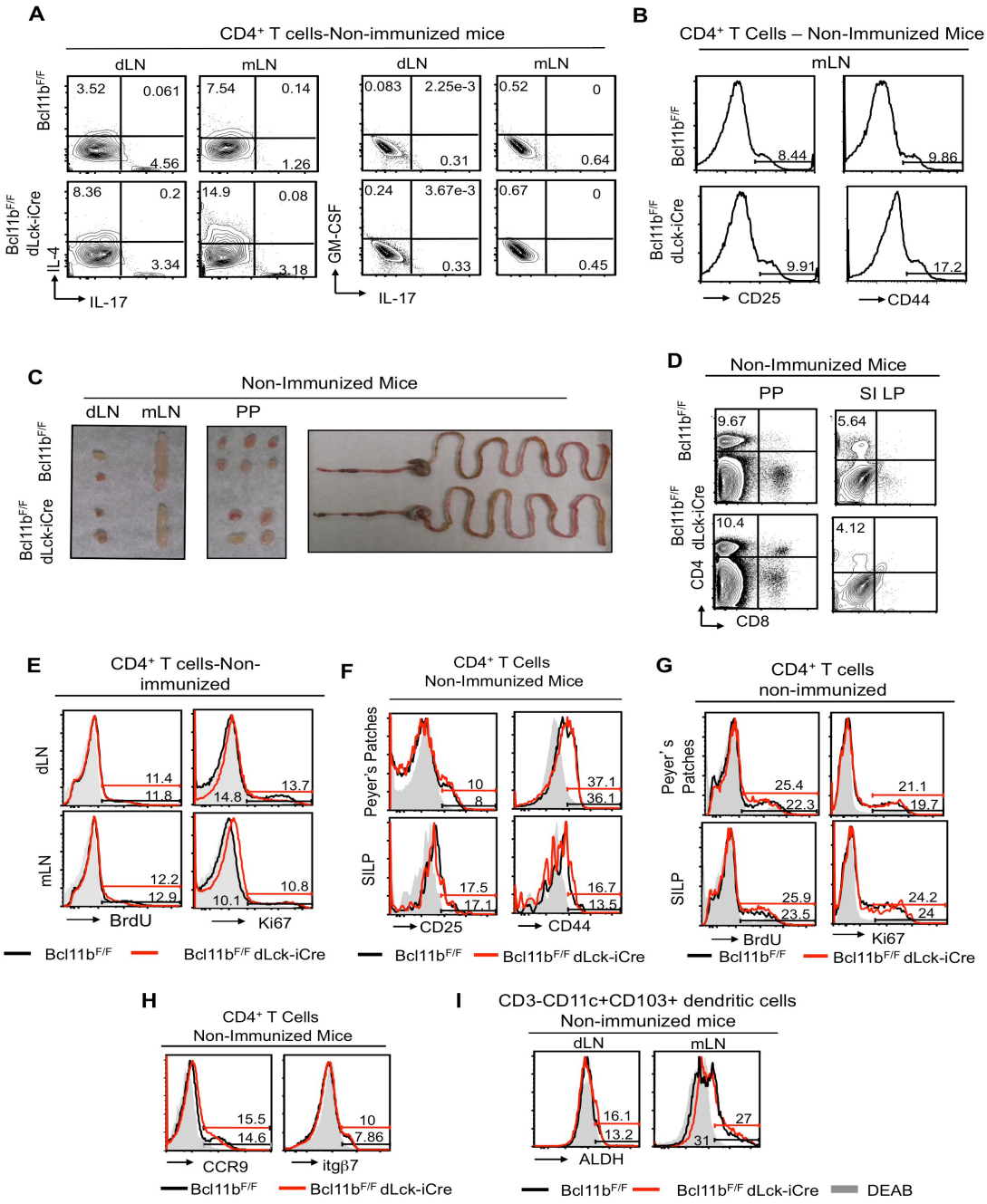

Figure S4. CD4$^+$ T cells of non-immunized Bcl11b$^{F/F}$/dLck-iCre mice. (A) FACS analysis of IL-17, GM-CSF and IL-4 production in CD4$^+$ T cells from the dLNs and mLNs of non-immunized Bcl11b$^{F/F}$/dLck-iCre and wild type mice. Data is representative of three pairs of mice. (B) Flow cytometry analysis of the activation markers CD25 (left) and CD44 (right) in CD4$^+$ T cells from mLNs of the indicated mice. (C) Gross anatomy of dLNs and mLNs, Peyer's patches, and intestine from the indicated mice. (D) FACS analysis of CD4$^+$ T cells in Peyer's patches (PP) and SILP of the indicated mice. (B-D) Data is representative of six pairs of mice. (E) Flow cytometry analysis of BrdU incorporation (left) and Ki67 levels (right) in the dLNs and mLNs of the indicated groups. Gray shaded area indicates negative control. Data is representative of three pairs of mice. (F) Flow cytometry analysis of the activation markers CD25 (left) and CD44 (right) in CD4$^+$ T cells from PP and SILP of the indicated groups. Gray shaded area represents negative control. Data is representative of six pairs of mice. (G) Same as in (E) in PP and SILP. (H) Flow cytometry analysis of CCR9 and itgβ7 on CD4$^+$ T cells of the indicated group. Gray shaded area represents negative control. (I) FACS analysis of ALDH activity in CD3$^-$CD11c$^+$CD103$^+$ dendritic cells of the indicated groups. Light gray shaded area represents samples treated with the inhibitor DEAB. Experiments conducted on mice 10-12 weeks of age.

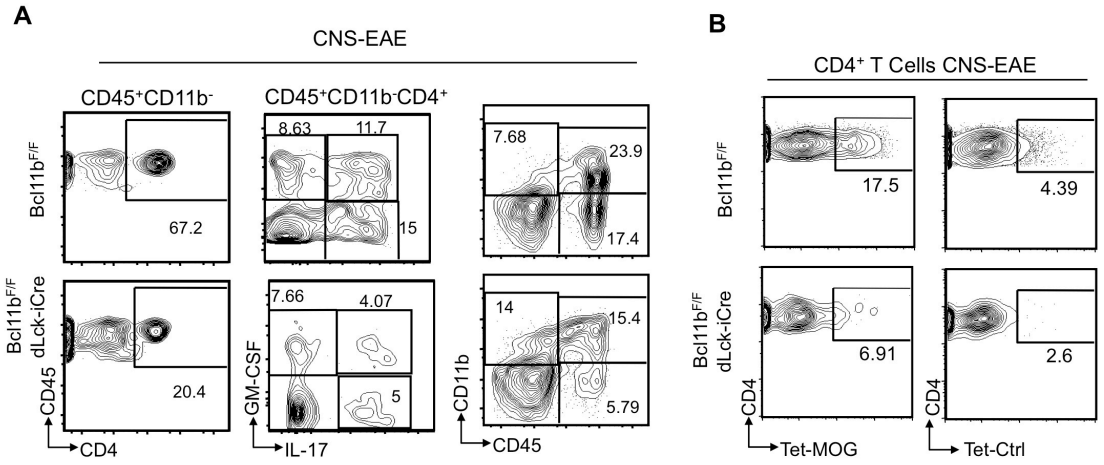

Figure S5. Frequencies of $CD4^{+}MOG_{35-55}{}^{+}$ T cells infiltrating the CNS were reduced in EAE $Bcl11b^{F/F}$/dLck-iCre mice, with the associated reduction in neuro-inflammation. (A) FACS analysis of $CD4^{+}CD45^{hi}$, $CD4^{+}IL\text{-}17^{+}GM\text{-}CSF^{+}$ T cells and $CD11b^{+}CD45^{hi}$ in the CNS of $Bcl11b^{F/F}$/dLck-iCre and wild type mice day 18 after EAE induction. Data is representative of three pairs of mice. (B) Frequencies of $CD4^{+}$MOG-specific (Tet-MOG) or a non-specific control (Tet-Ctrl) in CNS on day 18 post-EAE induction.

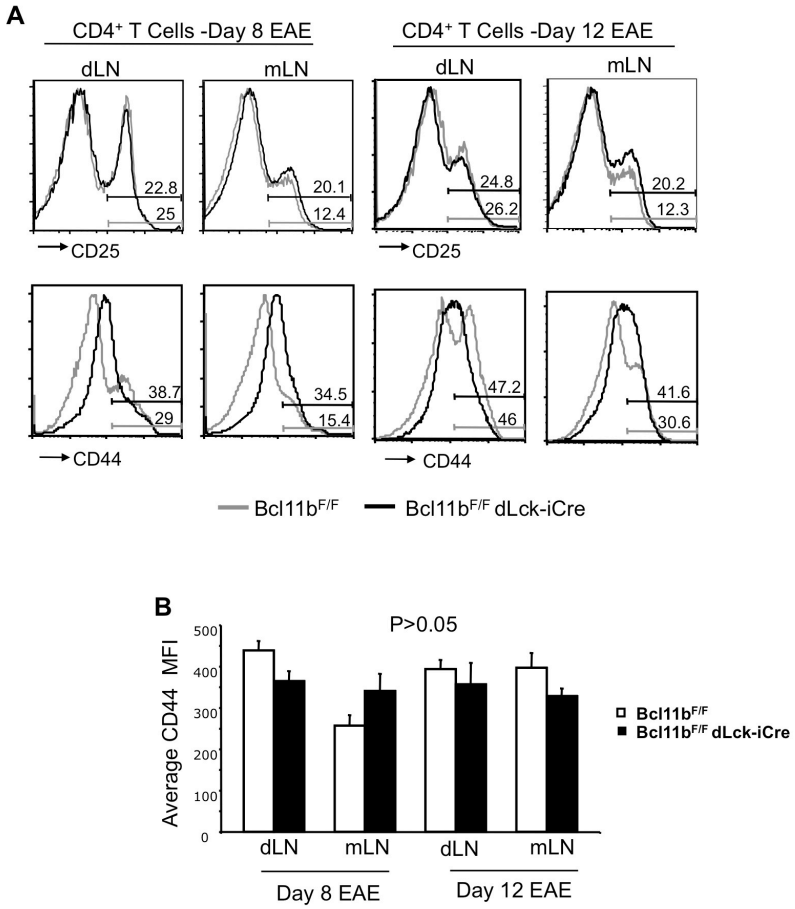

Figure S6. CD44 and CD25 on CD4$^+$ T cells from dLNs and mLNs of EAE Bcl11b$^{F/F}$/dLck-iCre mice and wild type mice on Days 8 and 12 post EAE induction. (A) Flow cytometry analysis of CD25 and CD44 on CD4$^+$ T cells from dLNs and mLNs of EAE Bcl11b$^{F/F}$/dLck-iCre (black) and wild type (gray) mice on day 8 (left) and day 12 (right) following EAE induction. (B) Average MFI for the CD44$^+$ population on CD4$^+$ T cells, in the dLNs and mLNs of EAE Bcl11b$^{F/F}$/dLck-iCre (black) and wild type mice (white), on the indicated days. p>0.05 for all as determined by two-tailed student's *t* test. Data is representative of four pairs of mice.

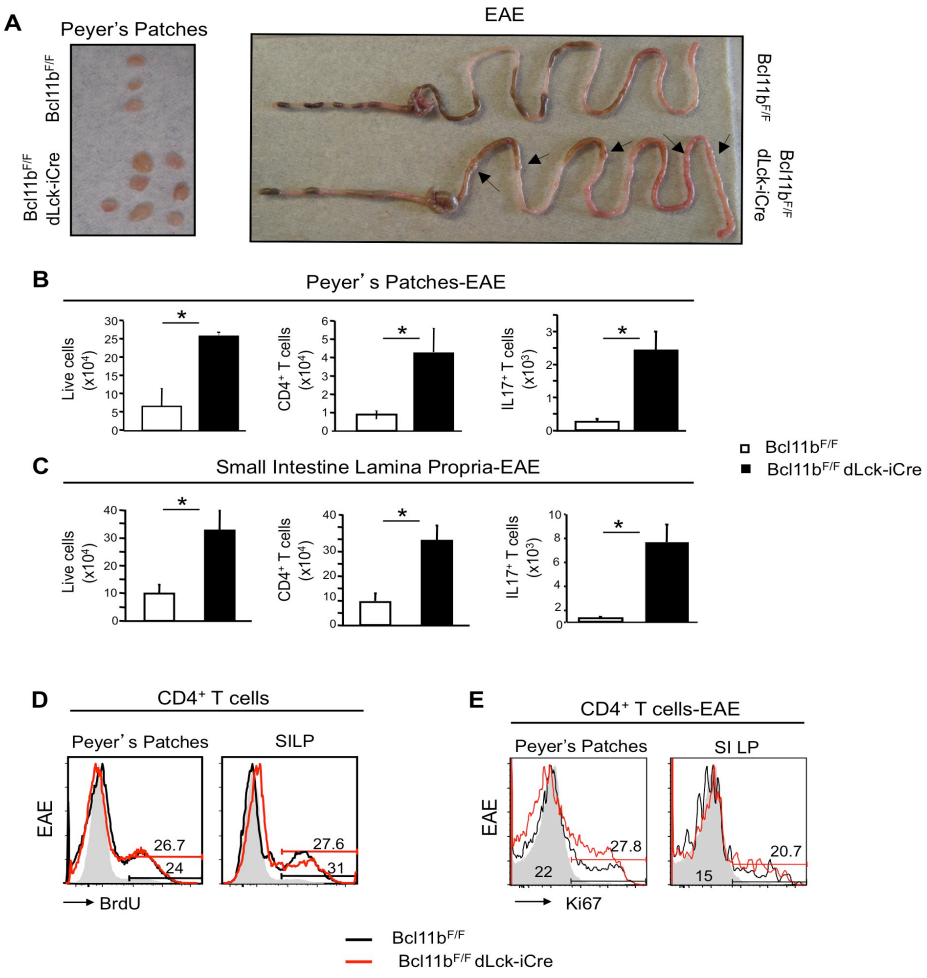

Figure S7. CD4$^+$ T cells accumulate in the Peyer's patches and small intestine in EAE Bcl11b$^{F/F}$/dLck-iCre mice, however they do no exhibit enhanced proliferation. (A) Peyer's patches and intestine gross anatomy of EAE Bcl11b$^{F/F}$/d Lck-iCre and wild type mice on day 18 after EAE induction. Black arrows indicate enlarged Peyer's patches on small intestine. Data is representative of 10 pairs of mice (B-C). Absolute numbers of live (left), CD4$^+$ T cells (center) and IL-17$^+$ CD4$^+$ T cells (right) in Peyer's patches (B) and small intestine lamina propria (C) of EAE wild type (white) and Bcl11b$^{F/F}$/dLck-iCre (black) mice on day 18 following EAE induction. Two-tailed student's *t* test was applied to determine significance. (B) (*p≤0.05, n=5) (mean ±SEM). (C) (*p≤0.05, n=6) (mean ±SEM). (D-E) FACS analysis of BrdU incorporation (D) and Ki67 levels (E) in the Peyer's patches and SILP of EAE Bcl11b$^{F/F}$/dLck-iCre (red) and wild type mice (black). Gray shaded area represents negative control. Data is representative of three pairs of mice.

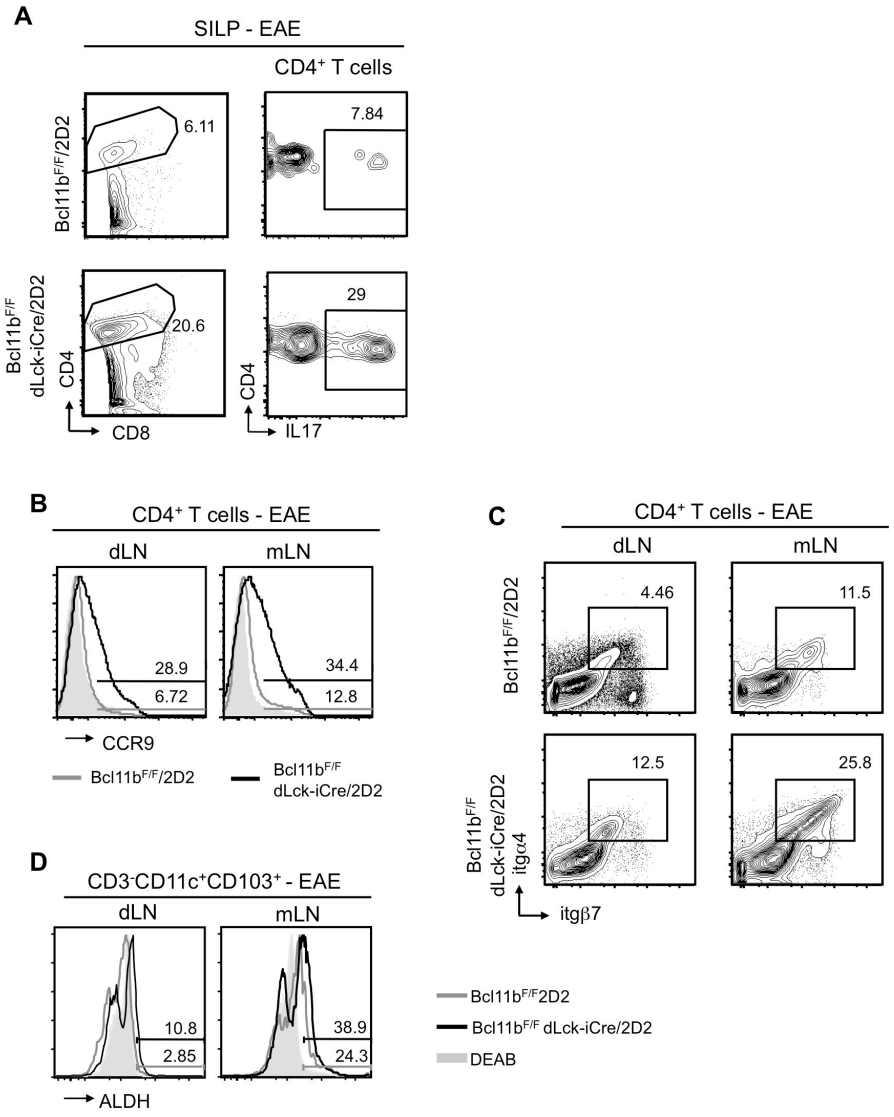

Figure S8. CD4$^+$ T cells of EAE Bcl11b$^{F/F}$/dLck-iCre/2D2 transgenic mice exhibited increased CD4$^+$ T cells accumulation in SILP, upregulation of gut homing markers on dLNs and mLNs and increased RALDH activity in dendritic cells. (A) Frequencies of CD4$^+$ T cells, and CD4$^+$IL-17$^+$ in small intestine lamina propria (SILP) of Bcl11b$^{F/F}$/dLck-iCre/2D2 and Bcl11b$^{F/F}$/2D2 on day 18 after EAE induction. (B-C) FACS analysis of CCR9 (B) and α4β7 (C) on CD4$^+$ T cells in dLNs and mLNs of Bcl11b$^{F/F}$/dLck-iCre/2D2 (black) and Bcl11b$^{F/F}$/2D2 (gray) mice on day 12 following EAE induction. (D) FACS analysis of ALDH activity in CD3$^-$CD11c$^+$CD103$^+$ dendritic cells from EAE Bcl11b$^{F/F}$/dLck-iCre/2D2 (black) and Bcl11b$^{F/F}$/2D2 (gray) mice on day 12 after EAE induction. Gray shaded area represents samples treated with DEAB inhibitor. In all histograms, gray shaded area represents negative control. Data is representative of four pairs of mice.

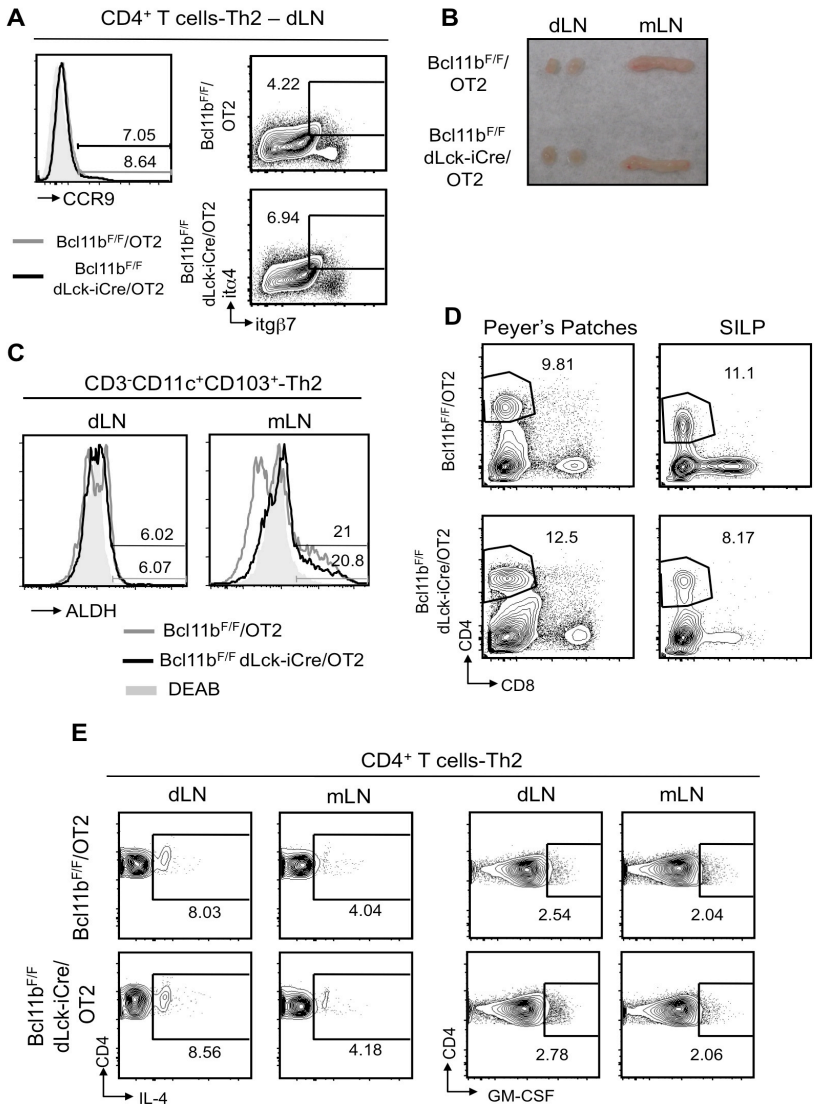

Figure S9. Bcl11b$^{F/F}$/dLck-iCre/OT2 mice immunized with OT2$_{323-339}$/Alum produce IL-4, but not GM-CSF, and do not upregulate gut homing markers or exhibit propensity of CD4^{+} T cells to accumulate into the gut. (A) FACS analysis of CCR9 and α4β7 levels on dLNs of CD4^{+} T cells from Bcl11b$^{F/F}$/dLck-iCre/OT2 (black) and Bcl11b$^{F/F}$/OT2 (gray) mice immunized with OT2$_{323-339}$/Alum plus Pam3CSK4, on day 8 post-immunization. (B) Gross anatomy of dLNs and mLNs of OT2$_{323-339}$/Alum immunized Bcl11b$^{F/F}$/dLck-iCre/OT2 and Bcl11b$^{F/F}$/OT2 mice on day 8 post-immunization. (C) FACS analysis of ALDH activity in CD3^{-}CD11c^{+}CD103^{+} dendritic cells from OT2$_{323-339}$/Alum immunized Bcl11b$^{F/F}$/dLck-iCre/OT2 (black) and Bcl11b$^{F/F}$/OT2 (gray), on day 8 post-immunization. Gray shaded area represents samples treated with DEAB inhibitor. (D) Frequencies of CD4^{+} T cells in Peyer's patches (left) and SILP (right) from Bcl11b$^{F/F}$/OT2 and Bcl11b$^{F/F}$/dLck-iCre/OT2 mice 8 days following immunization with OT2$_{323-339}$/Alum. (E) Frequencies of IL-4-producing (left) and GM-CSF-producing (right) CD4^{+} T cells in the dLNs and mLNs of Bcl11b$^{F/F}$/dLck-iCre/OT2 and Bcl11b$^{F/F}$/OT2 mice on day 7, following immunization with OT2$_{323-339}$/Alum. Data is representative of 3 pairs of mice.

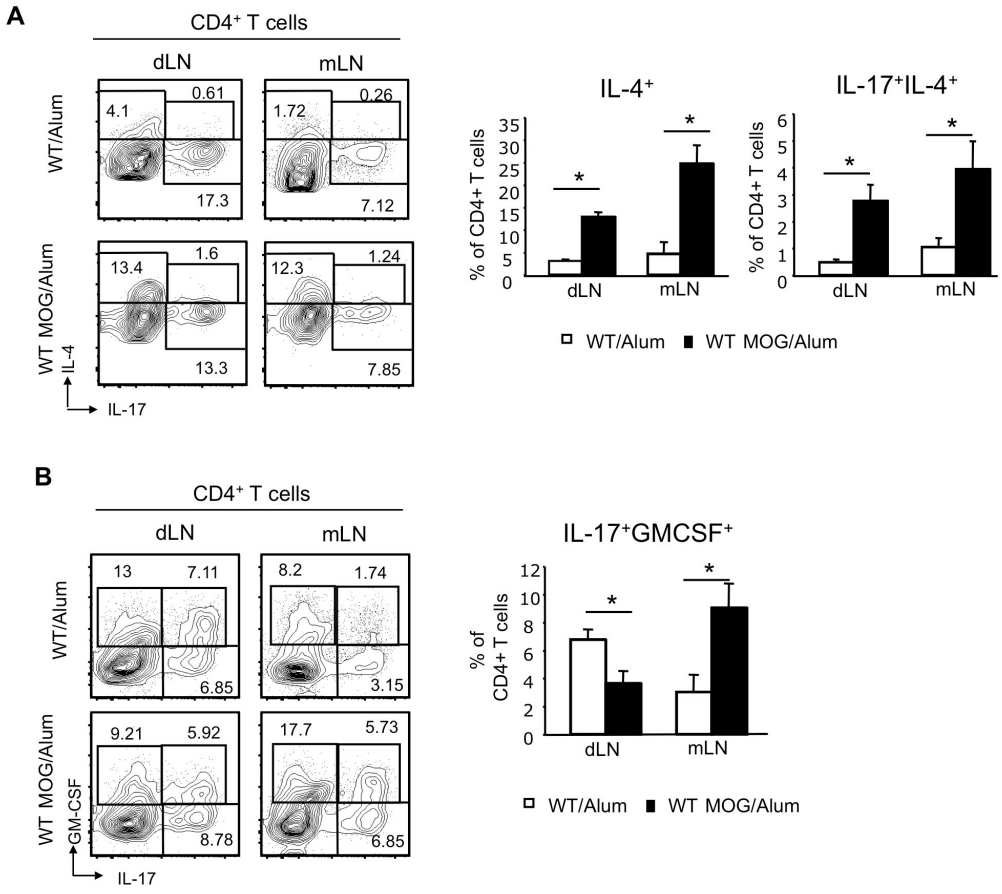

Figure S10. Treatment of EAE wild type mice with MOG/Alum induces production of IL-4 without inhibition of IL-17 and GM-CSF production. EAE wild type mice were treated with either MOG_{35-55} in alum, plus Pam3CSK4 (WT MOG/Alum), or alum alone (WT/Alum), day 7 post-EAE induction. (A-B) Flow cytometry analysis of IL-4 and IL-17 (A) and GM-CSF and IL-17 (B) (B) in gated $CD4^+$ T cells from dLNs and mLNs. Right panels show average frequencies of cytokine production in WT MOG/Alum and WT/Alum (*p≤0.05; n=5) (mean ±SEM).

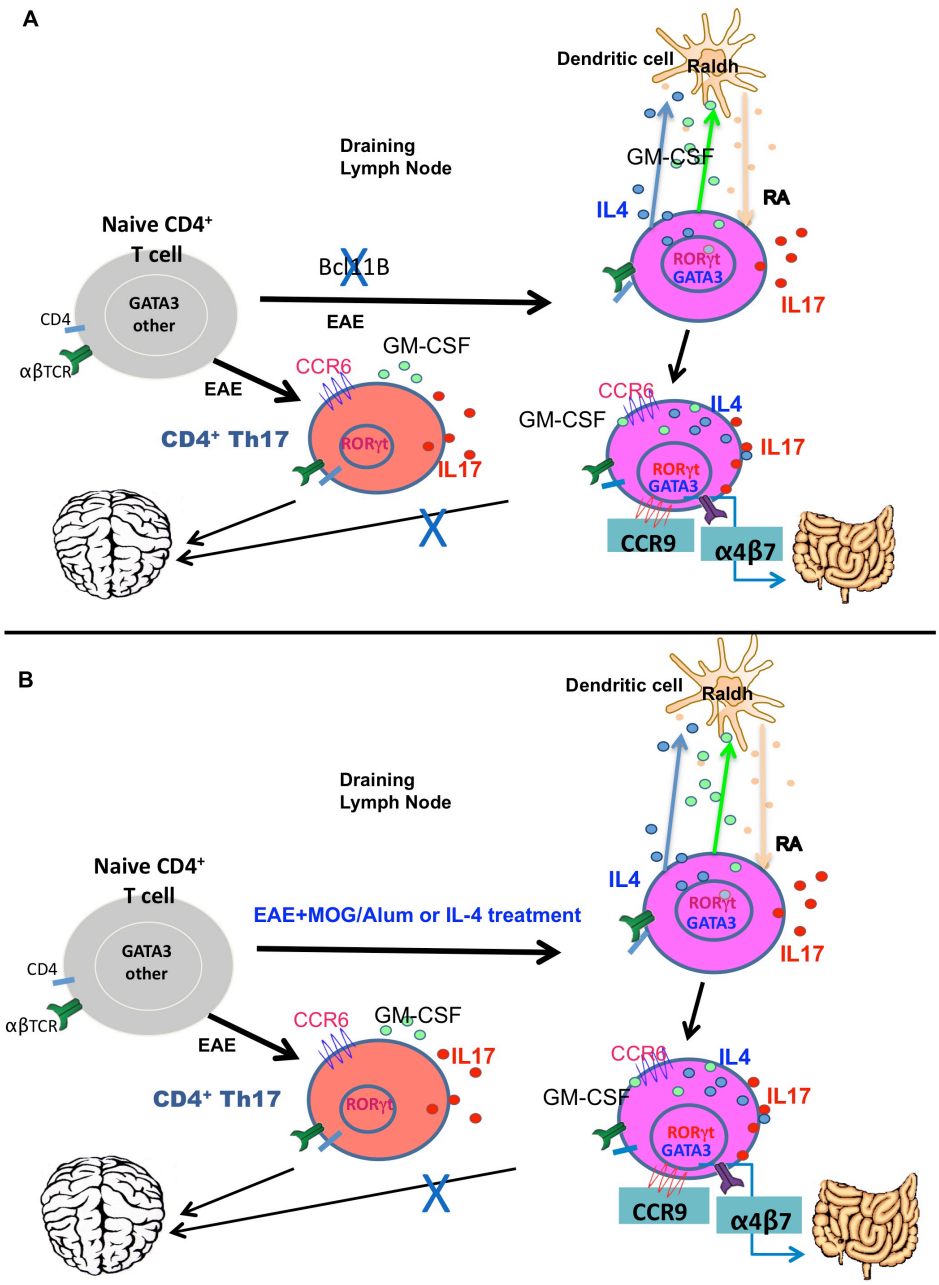

Figure S11. Model for re-routing of CD4$^+$ T cells from the dLNs/CNS to mLNs/gut through acquisition of a Th2 phenotype in Th17 cells following IL-4 induction during EAE. (A) During EAE induction, wild type CD4$^+$ T cells downregulated GATA3, upregulate Rorγt, which induces GM-CSF and IL-17 expression, upregulation of CCR6 and migration of CD4$^+$ T cells and other immune cells from the draining lymph nodes to the CNS. Bcl11b-deficient CD4$^+$ T cells fail to downregulate GATA3 following Th17 EAE response, however still express Rorγt. As a result, they produce IL-4, together with IL-17, and more importantly GM-CSF. Production of IL-4 together with GM-CSF results in the upregulation of RALDH2 expression and activity in dendritic cells, which produce elevated levels retinoic acid (RA). RA induces expression of CCR9 and α4β7 on T-helper cells, which causes their diverted migration away from dLNs-CNS route toward the mLNs-small intestine. This provides protection from EAE, despite the fact that these cells express normal levels of CCR6 and receptors for CNS entry. (B) The same process occurs without removal of Bcl11b, in conditions in which EAE induction in wild type mice is followed by immunization in Th2 conditions or treatment with IL-4.

SUPPLEMENTARY METHODS

Cell Isolation: $CD4^+$ T cells were isolated by negative selection using Dynal Mouse Negative Isolation kits (Invitrogen). Briefly, single cell suspensions were counted and resuspended in PBS containing 1% FBS and 0.5% EDTA. 20µl antibody mix per 1 x 10^7 cells were added to the cells, following by incubation at 4°C for 20 minutes. Magnetic beads were added to the washed cells, followed by incubation at room temperature for 15 minutes on a rotator. Unbound cells were then separated, and magnet bound cells were discarded. For lamina propria (LP) lymphocyte isolation, tissue was digested for 90 minutes in 0.750ml complete media (CM) containing 100 mg/ml collagenase D (Roche), 1mg/ml dispase II (Invitrogen), and 0.2-1 mg/ml DNAse (Roche). LP lymphocytes were further washed with CM and purified by 33% percoll gradient centrifugation. For brain and spinal cord lymphocyte isolation tissue was incubated in 2.5ml CM containing 25mg/ml collagenase D (Roche) and 1mg/ml DNAse (Roche). Cells were washed with CM and purified by 33% percoll gradient centrifugation.

Antibodies: Cells were surface stained with following antibodies: from eBioscience: anti-CD4 (clone GK1.5), anti-CD8a (clone 104), anti-CD25 (clone PC61.5), anti-CD3e (clone 17A2), anti-CD11a (clone M17/4), anti-CD11c (clone 3.9), anti-CD18 (clone M18/2), anti-CD29 (clone HMb1-1), anti-CD44 (clone IM7), anti-CD49d (clone RI-2), anti-CD103 (clone 2E7), anti-CCR9 (clone CW-1.2), anti-IL17 (clone ebio17B7), anti-IL4 (11B11), anti-CCR6 (clone 140 706), anti-itgβ7 (F1B504), anti-Rorγt (B2D); from

BD Biosciences: CD124 (clone mIL4R-M1), GATA3 (L50-823) Ki67 (B56) and anti-GM-CSF (MPI-22E9).

Evaluation of BrdU incorporation.

For BrdU incorporation, mice were administered 0.8mg/ml BrdU in their drinking water for seven days and sacrificed on day 8. Intranuclear staining followed surface staining, and was conducted using fixation and permeabilization buffers (eBioscience) with Protocol B. Previous to analysis for BrdU incorporation mice were administered 0.8mg/ml BrdU in their drinking water for seven days and sacrificed on the eighth day. BrdU (BU20A) staining was conducted as per manufacturers protocol (eBioscience).

Intracellular cytokine staining: Cells were stimulated for six hours with 50 ng/ml PMA and 500 ng/ml Ionomycin in CM at 37°C, with 10 μg/ml Brefeldin A. Cells were stained for surface markers, followed by fixation in 4% paraformaldehyde. Permeabilization of cells with 0.05% saponin buffer was performed before intracellular staining.

Flow Cytometry: Flow cytometry analyses were performed on a LSR or on FacsCalibur upgraded at three lasers and 8 colors (Cytek). Data was analyzed using FlowJo software (Tree Star Inc.)

Quantitative (q)RT-PCR: RNA was extracted using Trizol Reagent from $CD4^+$ or dendritic cells of EAE immunized mice and quantitative(q) RT-PCR was conducted as previously described[1]. The primers for qRT-PCR were chosen such as to extend products

under 200 bp, with no formation of primer dimmers, and cross introns. Sequence of the primers is available upon request. The relative abundance of each message was normalized to actin and calculated as: 2-(Ct gene-Ct actin), where Ct represents the threshold cycle for each transcript.

Tetramer Staining: Tetramer staining was conducted as described by Korn et al. [2]. Briefly, cells isolated from the CNS were stained with MOG_{35-55}/IAb tetramers or control (NIH Tetramer Core Facility, Emory University, Atlanta, GA) for three hours at room temperature, following incubation in serum-free media with 0.07μU/ml neuraminidase type X from Clostridium perfringens, at 37°C for 25 minutes. Cells were then stained with surface makers for 30 minutes at 4°C.

In vitro T helper polarization: Naïve $CD4^+$ T cells were purified from wild type and $Bcl11b^{F/F}$/dLck-iCre mice and were cultured on plate-bound anti-CD3 plates in ***Th0*** (anti-CD28(1μ/ml); IL-2(100U/ml)), ***Th1***(anti-CD28(1μ/ml); IL-2(100U/ml); IL-12(10ng/ml);anti-IL-4(10μg/ml)), ***Th2*** (anti-CD28(1μ/ml); IL-2(100U/ml); IL-4(5ng/ml); anti-IFNγ (10μg/ml);anti-IL-12(10μg/ml)), and ***Th17***(anti-CD28(1μ/ml); IL-6(10ng/ml); IL-21(20ng/ml); IL-23 (50ng/ml); IL1β (10ng/ml); TGF-β(5ng/ml) anti-IFNγ (10μg/ml); anti-IL-12(10μg/ml); anti-IL-4(10ug/ml)) conditions. Additionally cells were cultured in Th17 conditions without anti-IL-4. After four days, cells were removed from anti-CD3 and anti-CD28 but left in polarizing conditions for an additional three days. On day 7, cells were washed and restimulated with 50 ng/ml PMA and 500 ng/ml Ionomycin in CM

at 37°C, with 10 μg/ml Brefeldin A. Intranuclear and cytokine staining were conducted as described above.

Aldefluor Assay. To measure aldehyde dehydrogenase activity, we used an aldefluor assay kit from Stem Cell Technologies Inc. Cells were blocked and then kept in aldefluor assay buffer throughout experiment. 0.5μl aldefluor substrate was added to $1x10^6$ cells in 200 μl assay buffer in the presence or absence of 0.5μl of the inhibitor DEAB. All cells incubated at 37°C for 30 min, followed by staining for surface markers at 4°C for 15 min and FACS analysis.

In vitro RALDH activity assay: Dendritic cells were isolated from non-immunized CD45.1RAG2-/- mice and antigen loaded with 10μg/ml MOG_{35-55} followed by co-culture with purified $CD4^+$ T cells from EAE $Bcl11b^{F/F}$/dLck-iCre/2D2 and wild type 2D2 mice with or without the presence of anti-IL-4 (10μg/ml), anti-GM-CSF (10μg/ml) or both. After three days $CD45.1^+CD11c^+CD3^-$ dendritic cells were evaluated for RALDH activity using ALDEFLUOR assay as described above.

Histology. Upon euthanasia brain and spinal cord were fixed in 10% paraformaldehyde, paraffin embedded and sections were cut and stained with hematoxylin and eosin (H&E). Cross sections and stainings were performed by Mass Histology Service, Inc. Microscopic examination of the sections was performed using an Olympus BX51 instrument (Olympus).

Multiplex Bead Immunoassays: Equal numbers of purified $CD4^+$ and $CD8^+$ T cells were stimulated overnight with 50ng/ml PMA and 500 ng/ml Ionomycin, following which the supernatants were collected and immediately analyzed using a mouse multiplex fluorescent bead immunoassay (Millipore Inc). 50µl antibody coated beads were added to each duplicate well of a pre-wetted filter-bottom 96-well micro plate containing 25µl of sample, controls, or standard and incubated on shaker for 18-20 hrs at 4°C. After washing, 25µl of a solution containing a mixture of biotinylated, analyte-specific antibodies was added and incubated at room temperature for 1 hr, followed by washing and addition of 25µl streptavidin-PE and incubation on shaker for 30 min at room temperature and again washed three times. The plate was then read using a Luminex 100 instrument with a 5PL regression curve to plot the standard curve. Data analysis used Luminex xPONENT 3.1 Software. Mean fluorescence intensity of the samples was calculated based on a standard curve of known concentrations and expressed in pg/mL. Intra-assay precision was <5%CV and inter-assay precision determined using control samples was <10% for all cytokines.

SUPPLEMENTAL REFERENCES

1. Cismasiu, V.B.*, et al.* BCL11B participates in the activation of IL2 gene expression in CD4+ T lymphocytes. *Blood* **108**, 2695-2702 (2006).
2. Korn, T.*, et al.* Myelin-specific regulatory T cells accumulate in the CNS but fail to control autoimmune inflammation. *Nat Med* **13**, 423-431 (2007).